Axial Dispersion and Heat Transfer in Liquid-Liquid Spray Towers

F. O. MIXON, D. R. WHITAKER, and J. C. ORCUTT

Research Triangle Institute, Durham, North Carolina

A radiotracer technique was utilized to measure axial dispersion in both phases in spray towers operated at and near flooding. A new method that exhibits certain advantages over methods employed in the past is presented for reducing such data. It is demonstrated that axial dispersion in flooded and near-flooded spray towers is sufficiently severe to control completely their performance as heat exchangers.

The use of spray towers as liquid-liquid heat exchangers may be attractive for two reasons: First, the fouling problem can be largely avoided since there is no metallic surface in the heat transfer path to accumulate scale, and second, the resistance of the metallic path to heat transfer is eliminated. One must pay a price, however, in return for the removal of mechanical separation of the phases being contacted; that price is the ability to exert independent control over the flow characteristics within the contacting equipment. The flow characteristics of one phase are much more dependent on the presence of the other phase in direct contact equipment than in conventional shell-and-tube exchangers, in which mechanical separation is maintained. In particular, mixing patterns are induced in each phase as a result of contact with the other phase.

Several investigators (*16, 21*) have analyzed the effects of mixing on heat transfer by assuming that mixing in each phase can be characterized by an eddy thermal conductivity in that phase. Eddy diffusion terms are introduced into the differential mass balance equations, which are then transformed into dimensionless variables and are solved by one technique or another. Typical of the results so obtained are those of Sleicher (*21*) which indicate that the heat transfer efficiency to be expected from a contractor depends on the thermal capacitance flow ratio F, eddy Peclet numbers for both phases N_{Pe-o} and N_{Pe-w}, and the total number of transfer units T. For the special case $F = 1$, a portion of Sleicher's more comprehensive study can be represented as in Figure 1. In this figure, the abscissa can be regarded as a dimensionless local heat transfer coefficient or that representing the rate of heat transfer to an individual droplet. The ordinate can also be regarded as a dimensionless overall heat transfer coefficient, obtained from the logarithmic mean of the end values of ΔT. The parameter is an inverse composite measure of the mixing in both phases.

These results show that for no mixing, $\hat{N}_{Pe} = \infty$, the local and the overall heat transfer coefficients are equal, but that as mixing increases, $\hat{N}_{Pe} < \infty$, the overall average heat transfer coefficient is less than the local value. In other words, part of the potential heat transfer efficiency of the column is dissipated by mixing. It is interesting to note that for long columns, those characterized by large values of the abscissa, any mixing at all will tend to control the actual column performance. In other words, for long columns, column behavior as characterized by the apparent transfer units depends primarily on the average Peclet number or on the degree of mixing. Thus, so far as characterization of equipment performance is concerned, the Peclet numbers are at least as important as detailed knowledge of the local heat transfer behavior.

The question of local heat transfer, that is, that to individual droplets, has commanded the attention of many investigators (*6, 8, 10, 11, 14, 18*). This aspect of the problem is still far from being completely understood, but, as will be shown later, sufficient information is available to allow one in many cases to bracket actual column performance to those regions in which the long column approximation is quite realistic, that is, in which column

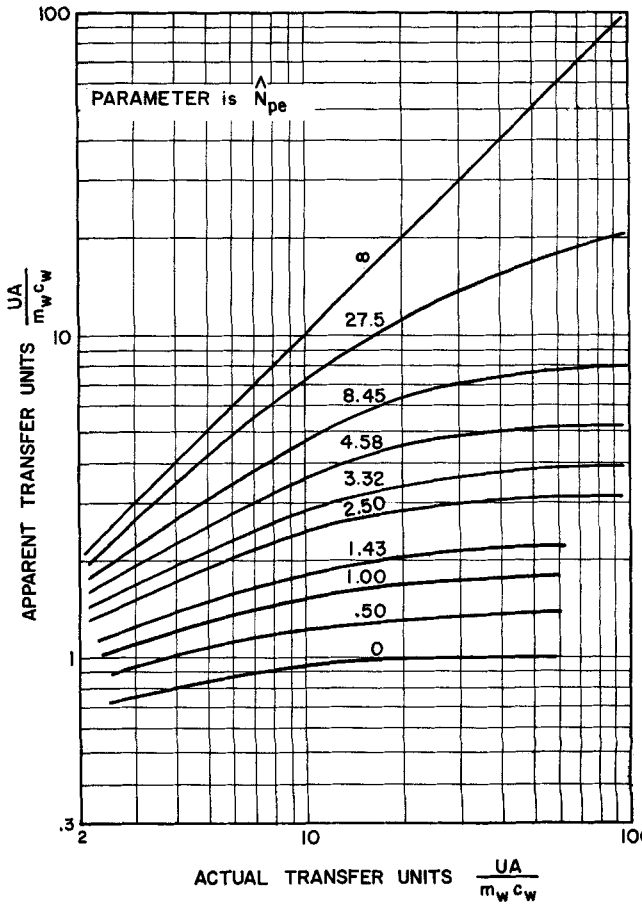

Fig. 1. The effect of mixing on heat transfer. Apparent transfer units vs. actual local transfer units for various values of average Peclet number.

performance is controlled by mixing rather than by local heat transfer rates.

Axial mixing in spray towers has also been studied by several investigators (*4, 9*). Brutvan (*4*) and Hazlebeck and Geankoplis (*9*) have measured continuous phase eddy diffusivities, but Brutvan utilized glass bead as the discontinuous phase and Hazlebeck and Geankoplis studied the low holdup region of operation. There appears to be a need for axial dispersion studies in regions of operation at or near flooding, that is, at larger holdups, as well as for both the continuous and the discontinuous phases.

MODES OF SPRAY-TOWER OPERATION

Consider a spray tower of the Elgin (*3*) type, shown schematically in Figure 2. The continuous phase is introduced into the top of the column and flows downward through the straight section, leaving from the bottom of the column. The discontinuous phase is dispersed through nozzles at the bottom of the column as droplets which then rise through the straight section to the coalescence zone at the top of the column.

For a fixed continuous phase flow rate, as the rate of dispersed phase flow is increased, the holdup of dispersed phase within the column increases simultaneously to the point at which more dispersed phase simply cannot be forced through the column. Any additional increase in the disperse phase flow will result in entrainment of droplets out the continuous phase exit. This mode of operation is usually designated as *flooding*.

To achieve this mode of operation, both flow rates must be at the flooding level, and the coalescence interface at the top of the column must be well away from the top of the straight section to permit free rise of the droplets into the coalescence zone. If the level of the coalescence interface is lowered to coincide with the top of the straight section, then (for some systems, at least) the droplets cannot freely escape into the coalescence zone and tend to pile up in the straight section with a holdup approaching that of close-packed spheres. The column can be operated stably at this condition, though at lower flow rates than those achieved in flooding in the usual sense. This second type of flooding will be designated as *close-packed flooding*.

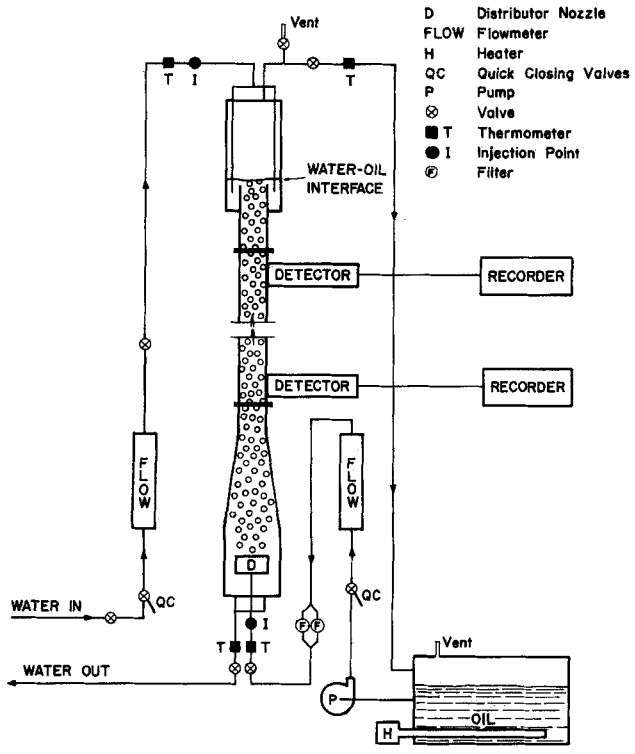

Fig. 2. Schematic diagram of Elgin column.

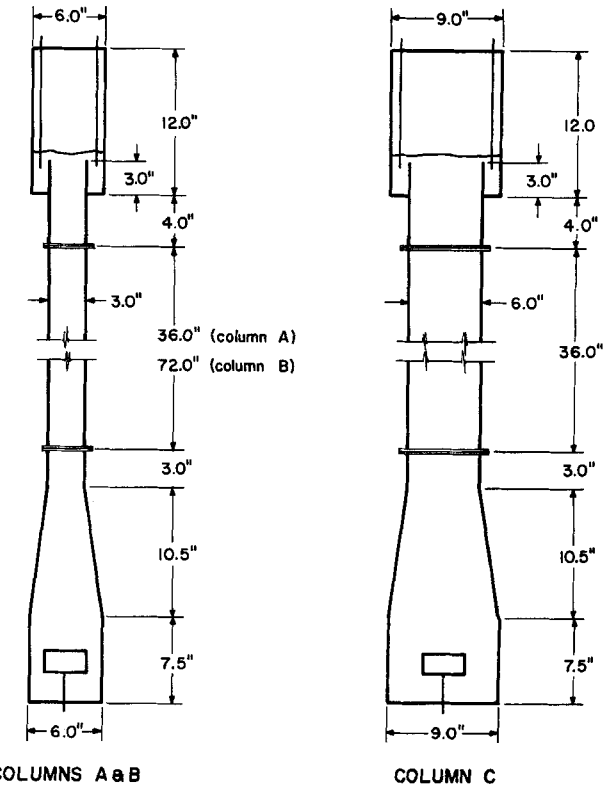

Fig. 3. Schematic drawing of the three experimental columns.

Studies of heat transfer behavior at nonflooded and flooded conditions have been reported by Sukhatme and Hurwitz (*22*); heat transfer at close-packed flooding has been reported by Woodward (*25*) and by Bauerle (*1*). This study is concerned with axial dispersion in both phases under these modes of column operation and upon the effects of this axial dispersion on heat transfer.

APPARATUS AND PROCEDURE

Average residence times and eddy Peclet numbers have been measured for spray towers operated in the flooded and near flooded range with a radiotracer technique. In all the cases, the continuous phase was water and the disperse phase was a light, water-insoluble oil of density 49 $lb._m$/cu.ft., heat capacity 0.48 B.t.u./$lb._m$)(°F.), thermal conductivity 0.08 B.t.u./(hr.)(ft.)(°F.), and viscosity 1.5 centipoise, all at room temperature. Three different columns were studied; their dimensions are as indicated in Figure 3.

The radiotracer was indium-113m,* prepared by the procedure of Mayer and Anderson (*13*). For water phase tracing, an acid solution of the isotope was utilized; for oil phase tracing, the isotope was extracted with 0.25 M thenoyltriflouroacetone in benzene. Counting was accomplished with Nuclear Chicago Model DS-5 Scintillation Counters in conjunction with Nuclear Chicago Model 185 Scalers and Model 1620B Ratemeters for conversion of the digital pulses to analog signals. Counting rates were recorded on strip-chart recorders.

A single run involved bringing the column to steady state operation, injecting a pulse of tracer into either the oil or water feed stream, and then monitoring the passage of tracer across two measurement planes located as indicated in Figure 2. Flooding, near flooding, and close-packed flooding conditions were investigated with tracer injected into both continuous and disperse phases. In all cases, the oil rate was adjusted to

* Metastable.

2.5 times the water rate (this corresponds to equal thermal capacitance flow rates for the two phases, $m_o c_o = m_w c_w$).

TREATMENT OF THE DATA

It was originally planned to reduce the data by the moments method described by Bischoff and Levenspiel (2). This method necessitates calculation of the mean and variance of a signal at each of two observation points. The average residence time and the Peclet number are then calculable from the differences in the means and the variances of the signal at the two observations points.

A practical difficulty arose, however, that causes this method to be less attractive than was originally anticipated. Radiotracer, after being injected into the column feed (particularly the water feed), tended to stagnate in the coalescence zone of the column and to be washed out very slowly. The effect of this behavior was to cause the counting rate vs. time signals to have long and uncertain tails. This caused the variances of the signals at the two measurement points to be quite large and somewhat uncertain, and the Peclet number depends on the difference of these variances. The net effect seemed to be that far too much emphasis in the data reduction was being accorded to the most uncertain portion of the data, namely, the signal tails rather than the regions of maximum counting rate.

In a recent paper, Sater and Levenspiel (20) fitted the tails of the measured distributions with decaying exponential functions and then used quadrature to establish the contributions of these exponential tails to the first and second moments. Regardless of the care used in evaluating the contributions of the tails, these contributions are still large compared to the contributions of the regions of maximum counting rate, and too much weight in the data reduction is still given to the most uncertain part of the data.

To minimize these problems, a modification of the moments method was developed with the purpose of providing a better method of treating concentration time curves with large variances. Details of the development are included in the Appendix. In the Appendix it is shown that to compute τ and N_{Pe-o} or N_{Pe-w} from the data, one selects a value for k' more or less arbitrarily and then computes the zeroth and first moments of the modified function $c \exp - k't$ at each of the measurement points. Values of τ and N_{Pe-o} or N_{Pe-w} are then directly calculable from these moments.

It can be shown that this method is related to that of Bischoff and Levenspiel (2) in the following sense. If one sets k' equal to zero, then the present method becomes indeterminate. In the limit as k' tends to zero, however, the method reduces to that of Bischoff and Levenspiel (2) or of Sater and Levenspiel (20).

The more general method has several advantages over the more restricted method previously used. First, the new method involves calculation of the zeroth and first moments rather than of the first and second moments. Since the higher moments magnify the uncertainties in the tails of the distributions, it is advantageous to avoid the second moment. Second, the degree of emphasis accorded to various portions of the response curves can be shifted by changing k'. For small k', the method accords more emphasis to the tails of the distributions, and as k' is increased, the emphasis shifts toward the short-time portion of the curves. Repetition of the data reduction for several values of k' will then give results in which various portions of the data are emphasized, that is, in which the specific shapes of the measured distributions are brought into consideration. To illustrate this point, consider two distributions which do not happen to be related by the appropriate convolution integral, that is, that are not consistent with the assumed diffusion model. If τ and N_{Pe} are determined from these distributions by the method of Bischoff and Levenspiel (2), one gets no idea of the inconsistency with the assumed model. On the other hand, if τ and N_{Pe} are determined by using several values of k', the agreement or disagreement among the separate determinations affords an estimate of the degree of consistency of the data with the assumed model. Third, the method described here is capable of handling, for example, step inputs, whereas that of Bischoff and Levenspiel is not (the variances are infinite).

TABLE 1. RESULTS OF SMALL CORRECTION TO BACKGROUND RADIATION LEVEL. RUN NO. 1, WATER PHASE MEASUREMENT

k', min.$^{-1}$	τ, min.	τ(corr.), min.	N_{Pe-w}	N_{Pe-w} (corr.)
0.25	1.28	1.26	10.1	15.4
0.50	1.33	1.30	5.3	6.5
1.00	1.39	1.34	4.1	5.1
1.50	1.43	1.33	3.6	5.3
2.00	1.51	1.28	3.1	6.2
2.50	1.71	1.20	2.3	8.3
3.00	2.31	1.07	1.4	15.4

Two corrections were applied to the raw data prior to calculation of the moments and then the average residence time and the Peclet number. First, the background laboratory radiation level was subtracted from the measured signals; second, the signals were corrected to account for the radioactive decay of the tracer during the time of transit between the two measurement points.

A difficulty arose in connection with the reduction of the data that necessitated special attention to the background radiation level. If the data were, in fact, consistent with the assumed diffusion model, and if the proper value for background radiation level were known, then one would expect that calculated results for a particular run should be independent of the choice of the parameter k'. However, it was found that if the data were reduced by using as a background correction that which was estimated directly from the strip chart recorders, calculated values of τ and N_{Pe-o} showed a definite trend with k'. It was suspected that this observed trend was the result of insufficient precision in the estimation of the background radiation level. To test this idea, the calculations were repeated by assuming different background levels, looking for the level that resulted in the most nearly constant values of N_{Pe} as a function of k'. Considerable improvement was found in the apparent consistency of the data with rather small adjustments to the background radiation level. In most cases, the necessary adjustment to the background radiation level proved so small as to be indistinguishable on the strip-chart recorders. Typical results of such an adjustment are shown in Table 1.

After these corrections, a slight trend of both τ and N_{Pe} with k' still existed, even though the resulting values were those most consistent with the data and the diffusion model.

Uncorrected values resulted from a background radiation level of 0.042 as estimated from the recorder record. Corrected values resulted from a background level of 0.044, which corresponded to a minimum coefficient of variation of N_{Pe-w}.

It is seen that a trend of τ and N_{Pe} still exists, even though the values in Table 1 are presumably those most consistent with the data. That such a trend exists is probably indicative of inadequacies in the diffusion model in representing column behavior. Nonetheless, the diffusion model does afford acceptable characterization of the mix-

TABLE 2. WATER PHASE MEASUREMENTS

	Column C Straight sect. length / Diameter = 6			Column A Straight sect. length / Diameter = 12			Column B Straight sect. length / Diameter = 24		
	τ, min.	$N_{Pe\text{-}w}$	α_w, sq. ft./min.	τ, min	$N_{Pe\text{-}w}$	α_w, sq. ft./min.	τ, min.	$N_{Pw\text{-}w}$	α_w, sq. ft./min.
Flooding	0.71	0.52	10.8	1.26	8.0	0.36	3.7*	15*	0.4*
	0.39	0.99	10.4	1.5	3.4	0.72	2.5*	7*	1.28*
75%				1.7	2.5	0.86			
50%				1.28	1.29	2.2			
Close-packed flooding	0.54	0.7	10.6	0.8*	10*	0.46*	3.0*	10*	0.74*
				1.0*	10*	0.37*	3.0*	10*	0.74*

* The data from which these points were calculated exhibit a poor fit to the diffusion model. Tabular values should be regarded only as order-of-magnitude estimates.
__ Indicates seawater measurement.

ing behavior within the column, and even though the model may be inadequate in describing the detailed mechanism of the mixing operation, it should be serviceable in describing the overall effects of mixing on heat transfer behavior.

RESULTS

Experimental results for water phase measurements are listed in Table 2 and those for oil phase measurements are listed in Table 3. These results apply to the center portions of the columns only. Behavior in the end sections is probably quite different.

As is characteristic of axial dispersion measurements, there is quite a bit of scatter to the data. It is probable that some of the scatter can be attributed to the inadequacies of the diffusion model in representing the flow patterns and mixing behavior inside the spray tower, some to water surging, and some to the random nature of the mixing process.

Based upon the data, the following qualitative description of spray-tower mixing can be provided. At or near flooding, both phases exhibit behavior that is much nearer to the perfect mixing idealization than to the plug-flow idealization. This high degree of mixing results apparently from large swirls and recirculation patterns whose scale is on the order of a foot or more. As the column diameter is increased, the amount of oil phase mixing does not appear to change appreciably (the oil droplets still rise in about the same fashion as they do in small columns), but more mixing occurs in the water or continuous phase. Apparently the walls do not have the same effect in large columns in damping out the swirls and recirculation patterns as they do in small columns. More mixing occurs in close-packed flooding than in usual flooding. The oil droplets are mechanically restrained from free passage from the close-packed section, and, since they can't readily get out, they move around more.

At subflooding conditions, the discontinuous phase exhibits less mixing than at flooding, but the continuous phase exhibits more. This trend can be visualized by considering a column operated at very low throughput. For this mode of operation, the oil droplets will rise more or less uniformly to the top of the column with relatively little mixing, but the motion of these droplets will likely induce recirculation patterns in the water or continuous phase whose scale extends the entire length of the column. These large scale recirculation patterns result in a higher degree of mixing.

A MODEL FOR SPRAY-TOWER HEAT TRANSFER

Consider the heat transfer to a single droplet in a spray tower. According to the two-film theory, the heat flow can be regarded as in series through a continuous phase film resistance and then through a disperse phase film resistance. It is possible to make order-of-magnitude estimates of the individual film coefficients and hence of the overall local coefficient.

For the inside film, the coefficient of heat transfer must

TABLE 3. OIL PHASE MEASUREMENTS

	Column C Straight sect. length / Diameter = 6			Column A Straight sect. length / Diameter = 12			Column B Straight sect. length / Diameter = 24		
	τ, min.	$N_{Pe\text{-}o}$	α_o, sq. ft./min.	τ, min	$N_{Pe\text{-}o}$	α_o, sq. ft./min.	τ, min.	$N_{Pe\text{-}o}$	α_o, sq. ft./min.
Flooding	0.10	1.24	32.5	0.209	1.11	15.8	0.43	0.29	178
	0.083	1.16	41.5	0.179	0.66	31.1	0.43	0.48	108
				0.086	0.52	82			
				0.62	0.20	29.6			
75%				0.20	4.3	4.2			
				0.29	0.70	18.1			
50%				0.14	7.0	3.8	0.408	3.1	17.4
				0.21	1.3	13.5	0.38	4.7	12.4
							0.35*	15*	4.2*
Close-packed flooding	0.44	0.13	70	0.36	2.1				

* The data from which these points were calculated exhibit a poor fit to the diffusion model. Tabular values should be regarded only as order-of-magnitude estimates.

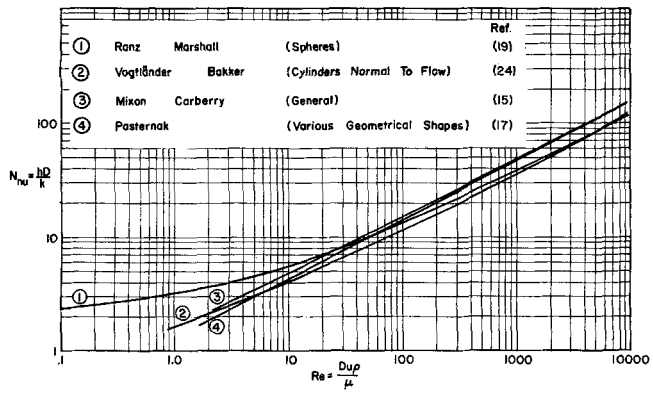

Fig. 4. Various correlations for outside Nusselt number.

be at least that which would occur if the internal heat transfer were by conduction alone with no convection whatever. From the analytic solution to the conduction problem for the interior of a sphere [given in analytic form (5) and in graphical form (23)], it follows that pure conduction corresponds to

$$N_{Nu} = \frac{hd}{k} = \frac{2\pi^2}{3} = 6.5$$

This Nusselt number, however, is unrealistically low, since there is convection within the droplets as described by Hadamard (7). Kronig and Brink (11) have analyzed heat transfer in the presence of Hadamard recirculation patterns and have shown that one should expect the value for N_{Nu} to equal about 17.6 rather than the lower value characteristic of conduction alone. Furthermore, according to Handlos and Baron (8), turbulent mixing also occurs within the interior of the drop which can lead to Nusselt numbers much higher than 17.6. Experimental mass transfer studies on single droplets by Johnson and Hamielec (10) confirm that for heat transfer, one should expect the internal Nusselt number to be higher than the Kronig-Brink value. It thus appears that one should expect the internal film coefficient to be at least that corresponding to a Nusselt number of 17.6 and in most cases somewhat higher.

A collection of several correlations applicable to the outside film is given in Figure 4. For usual conditions of operation of spray towers, the Reynolds numbers are in the range from 100 to 1,000. It is apparent from the figure that under these conditions, one should expect the value of an outside Nusselt number to be at least 10.

Assuming a drop diameter of 0.2 in., one would expect at least the following values for the film heat transfer coefficients:

For the inside film: h = 82 B.t.u./(hr.)(sq. ft.)(°F.)
For the outside film: h = 210 B.t.u./(hr.)(sq. ft.)(°F.)
For both films: U = 60 B.t.u./(hr.)(sq. ft.)(°F.)

These values represent rather conservative estimates as to what one might expect the local heat transfer behavior to be. It seems quite likely that more realistic estimates might produce a local coefficient of around 200 B.t.u./(hr.)(sq. ft.)(°F.)

With this value of the local coefficient, again by assuming droplets 0.2 in. in diameter and a 50% column holdup at flooding, the number of transfer units in a flooded 3-ft. column is about 15.

By referring to Figure 1, it can be seen that for low values of the Peclet numbers, the number of apparent transfer units differs very little from that corresponding to an infinite number of actual transfer units. In fact, for both oil and water Peclet numbers of 5, and $UA/m_wc_w = 10$, the solution differs from that for $UA/m_wc_w = \infty$ by less than 8%. The assumption that $UA/m_wc_w = \infty$ should then be a reasonable approximation for cases of practical interest.

The assumption that $UA/m_wc_w = \infty$ is equivalent to assuming that at any point within the spray tower, the discontinuous and continuous phases are in thermal equilibrium ($U = \infty$). Then there is only a single column temperature at any point within the column proper; this temperature distribution is described by the differential equation

$$(k_o + k_w)\, A_c \frac{d^2T}{dx^2} + (m_wc_w - m_oc_o)\frac{dT}{dx} = 0 \quad (1)$$

In this equation, the first term represents the net heat transfer to a differential element by eddy diffusion in both phases, and the second term represents the net convective transport of heat. The boundary conditions are

$$T = T_i - \frac{(k_w + k_o)}{m_wc_w} A_c \frac{dT}{dx} \text{ (top of column)} \quad (2)$$

and

$$T = \theta_i + \frac{(k_o + k_w)}{m_oc_w} A_c \frac{dT}{dx} \text{ (bottom of column)} \quad (3)$$

By introducing the following dimensionless variables

$$\eta = \frac{T - T_i}{\theta_i - T_i}$$

$$\zeta = x/L$$

$$F = m_wc_w/m_oc_o$$

$$N_{Pe-o} = L\,u_o/\alpha_o$$

$$N_{Pe-w} = L\,u_w/\alpha_w$$

the differential equation and boundary conditions become

$$\left(\frac{1}{\hat{N}_{Pe}}\right)\eta'' + (F-1)\,\eta' = 0 \quad (4)$$

$$\eta(1) = -\frac{1}{F}\left(\frac{1}{\hat{N}_{Pe}}\right)\eta'(1) \quad (5)$$

$$\eta(0) = 1 + \left(\frac{1}{\hat{N}_{Pe}}\right)\eta'(0) \quad (6)$$

with solution

$$\eta(\zeta) = \frac{-E}{F^2 - E} + \frac{F}{F^2 - E}\exp\left[(1-F)\,\hat{N}_{Pe}\right]\zeta \quad (7)$$

$$E = \exp\left[(1-F)\,\hat{N}_{Pe}\right] \quad (8)$$

It is seen that under the assumption of no local resistance to heat transfer, the behavior of the column depends only on two parameters, F and $\hat{N}_{Pe}$, the latter of which can be regarded as an average Peclet number which serves to characterize the contribution of diffusion in both phases to the overall column performance. This particular description of spray-tower heat transfer represents a special case of a more general set of results given by Miyauchi (16) and also a limiting case of the open-open model discussed by Levenspiel (2).

COMPARISON WITH OTHER STUDIES

If, as argued in the preceding section, the heat transfer behavior depends only on the parameters F and $\hat{N}_{Pe}$,

then it is possible to calculate the latter of these parameters from measurements in inlet and outlet temperature on spray-tower heat exchangers. This has been done from the heat transfer measurements of Sukhatme and Hurwitz (22) for holdups in excess of about 20%. The results are shown, together with values estimated from our axial dispersion measurements, in Figure 5. In this figure, a range of values for $\hat{N}_{Pe}$ is given for each value of F. This uncertainty is present, in the case of the Sukhatme and Hurwitz measurements, because of heat losses from the column. Consequently, values for $\hat{N}_{Pe}$ calculated from the water efficiency will be different than those calculated from the oil efficiency. The differences are as indicated in the figure.

Letan and Kehat (12) have recently reported experimental measurements of the temperature jump experienced by the continuous phase immediately upon entering the column. The diffusion model adopted in this report predicts such a jump and furthermore states that the magnitude of the jump depends on the parameters F and $\hat{N}_{Pe}$. From these temperature jump measurements, then, values of the diffusion parameter are back-calculated, are scaled to a column length corresponding to that of this report and of Sukhatme and Hurwitz, and are also shown for comparison in Figure 5.

Figure 5, then, shows a composite of data deduced from three different types of measurements: those of Sukhatme and Hurwitz, who measured inlet and outlet temperatures; those of Letan and Kehat, who measured the local temperature jump of entering continuous phase, and those of this report, which gives axial dispersion directly. The agreement among the three types of data lends confirmation to our hypothesis that the heat transfer behavior of spray columns operated in the near-flooded range depends almost entirely on the mixing characteristics in the column and to a very small extent on the local rate of heat transfer.

The data of Figure 5 were all taken on small columns, approximately 3 in. in diameter and 6 ft. long. It would be interesting to know of the dependence of $\hat{N}_{Pe}$ on column length and diameter. The measurements reported herein are not sufficiently precise to permit any conclusive statements to be made, but, if anything, N_{Pe-o} remains constant or increases slightly with column diameter and appears to be independent of column length. N_{Pe-w} exhibits a significant decrease with increasing column diameter over the diameter range from 3 to 6 in. Generally, both N_{Pe-o} and N_{Pe-w} seem lower for close-packed flooding than for flooding in the usual sense.

The value of $\hat{N}_{Pe}$ decreases somewhat as diameter increases. Just how strong this dependence is remains uncertain, but the data indicate that $\hat{N}_{Pe}$ is approximately halved for a twofold increase in diameter from 3 to 6 in. This trend, however, should not be extrapolated, since it likely that mixing behavior becomes independent of column diameter for large diameter columns.

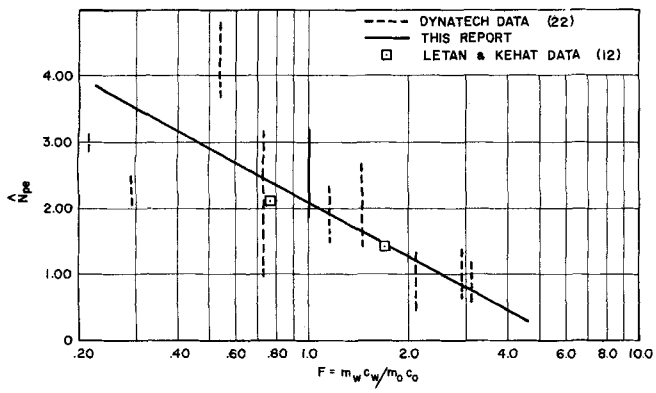

Fig. 5. Measured and calculated values of average Peclet number.

Values of N_{Pe-w} tend to be higher at flooding than at subflooding conditions; on the other hand, values of N_{Pe-o} are higher at subflooding conditions.

Several runs were made by using seawater rather than city water. The results indicate no particular difference between the behavior of the system operating on seawater and that with fresh water.

For small columns, a satisfactory correlation of the data appears to be that indicated in Figure 5. The equation of the straight line drawn by eye through the data is

$$\hat{N}_{Pe} = 2.06 - 1.20 \ln F \qquad (11)$$

For large columns (in excess of 6 in. in diameter), no data are available.

ACKNOWLEDGMENT

This work was carried out under the sponsorship of the U. S. Department of the Interior, Office of Saline Water. The assistance of B. R. Roberts and K. L. Fletcher with the experimental work is greatly appreciated.

NOTATION

A = area for heat transfer, sq. ft.
A = α_o/α_i
A_c = cross-sectional area for heat transfer, sq. ft.
B = $\beta_o/\alpha_o - \beta_i/\alpha_i$
c = radiotracer concentration or counting rate, arbitrary units
c_w = water heat capacity, B.t.u./(lb.$_m$)(°F.)
c_o = oil heat capacity, B.t.u./(lb.$_m$)(°F.)
d = droplet diameter, ft.
E = exp $[(1 - F)N_{Pe}]$
F = ratio of thermal capacitance flows, $m_w c_w/m_o c_o$
h = local heat transfer coefficient, B.t.u./(hr.)(sq. ft.)(°F.)
$I(s)$ = Laplace transform of counting rate at upstream measurement point
k = thermal conductivity, B.t.u./(hr.)(sq. ft.)(°F.) or arbitrary parameter for data reduction; see Appendix
k' = k/τ
k_o = eddy thermal conductivity of oil, B.t.u./(hr.)(sq. ft.)(°F.)
k_w = eddy thermal conductivity of water, B.t.u./(hr.)(sq. ft.)(°F.)
L = distance between measurement points, ft.
m_o = mass rate of oil, lb.$_m$/hr.
m_w = mass rate of water, lb.$_m$/hr.
N_{Nu} = Nusselt number, hd/k
N_{Pe-o} = oil phase Peclet number based on length between measurement points, Lu_o/α_o
$\hat{N}_{Pe}$ = average Peclet number, $\dfrac{N_{Pe-o}\,N_{Pe-w}}{N_{Pe-w} + F\,N_{Pe-o}}$
N_{Pe-w} = water phase Peclet number based on length between measurement points Lu_w/α_w
$O(s)$ = Laplace transform of counting rate at downstream measurement point
s = Laplace transform variable
t = time, min.
T = number of transfer units, $UA/m_w c_w$ dimensionless; also temperature, °F.
T_i = inlet water temperature, °F.
U = overall heat transfer coefficient, B.t.u./(hr.)(sq.

ft.) (°F.)

u_o = oil superficial velocity, ft./min.

u_w = water superficial velocity, ft./min.

x = distance along column, ft.

Z = modified counting rate, $c \exp - kt$

Greek Letters

α_i = zeroth moment of Z function at upstream measurement point; see Equation (A-16), Appendix A

α_o = zeroth moment of Z function of downstream measurement point; see Equation (A-14), Appendix A

α_o = oil phase eddy thermal diffusivity, sq. ft./min.

α_w = water phase eddy thermal diffusivity, sq. ft./min.

β_i = first moment of Z function at upstream measurement point; see Equation (A-18), Appendix A

β_o = first moment of Z function at downstream measurement point; see Equation (A-17), Appendix A

ζ = dimensionless distance variable, x/L

$\eta(\zeta)$ = water phase efficiency at ζ, $\dfrac{T - T_i}{\theta_i - T_i}$

θ = dimensionless time variable, T/τ

θ_i = inlet oil temperature, °F.

τ = average residence time between measurement points, min.

ρ = density, lb.$_m$/cu. ft.

LITERATURE CITED

1. Bauerle, G. L., *Ind. Eng. Chem. Proc. Design Develop.*, 225 (1965).
2. Bischoff, K. B., and O. Levenspiel, *Chem. Eng. Sci.*, **17**, 245 (1962).
3. Blanding, F. H., and J. C. Elgin, *Trans. Am. Inst. Chem. Engrs.*, **38**, 305 (1942).
4. Brutvan, D. R., Ph.D. dissertation, Rensselaer Polytech. Inst., Troy, N. Y. (1958).
5. Carslaw, H. S., and J. C. Jaeger, "Conduction of Heat in Solids," 2 ed., Clarendon Press, Oxford (1959).
6. Constan, G. L., and Seymour Calvert, *A.I.Ch.E. J.*, **9**, 109 (1963).
7. Hadamard, J., *Compt. Rend.*, **152**, 1735 (1911).
8. Handlos, A. E., and T. Baron, *A.I.Ch.E. J.*, **3**, 127 (1957).
9. Hazlebeck, D. E., and C. J. Geankoplis, *Ind. Eng. Chem.*, **2**, 210 (1963).
10. Johnson, A. I., and A. E. Hamielec, *A.I.Ch.E. J.*, **6**, 145 (1960).
11. Kronig, R., and J. C. Brink, *Appl. Sci. Res.*, **A-2**, 142 (1950).
12. Letan, Ruth, and Ephraim Kehat, *A.I.Ch.E. J.*, **11**, 804 (1965).
13. Mayer, W. J., and R. L. Anderson, *Ind. Eng. Chem.*, **52**, 993 (1960).
14. McDowell, R. V., and J. E. Myers, *A.I.Ch.E. J.*, **2**, 384 (1956).
15. Mixon, F. O., and J. J. Carberry, *Chem. Eng. Sci.*, **13**, 30 (1960).
16. Miyauchi, Terukatsu, *U.S.A.E.C. Rept. No. UCRL-3911* (1957).
17. Pasternak, I. S., and W. H. Gauvin, *Can. J. Chem. Eng.*, **38**, 35 (1960).
18. Popovich, A. T., R. E. Jarvis, and O. Trass, *Chem. Eng. Sci.*, **19**, 357 (1964).
19. Ranz, W. E., and W. R. Marshall, *Chem. Eng. Progr.*, **48**, 141 (1952).
20. Sater, V. E., and O. Levenspiel, *Ind. Eng. Chem. Fundamentals*, **5**, 86 (1966).
21. Sleicher, C. A., *A.I.Ch.E. J.*, **5**, 145 (1959).
22. Sukhatme, S. P., and M. Hurwitz, *Rept. No. 465*, Dynatech Corp., Office of Saline Water (Sept., 1964).
23. Treybal, R. E., "Mass Transfer Operations," McGraw-Hill, New York (1955).
24. Vogtlander, P. H., and C. A. P. Bakker, *Chem. Eng. Sci.*, **18**, 583 (1963).
25. Woodward, T., *Chem. Eng. Progr.*, **57**, 52 (1961).

APPENDIX A: DERIVATION OF METHOD OF DATA REDUCTION

The differential equation which describes the concentration or counting rate spatial and temporal dependence in the presence of diffusional transport is

$$\frac{\partial c}{\partial \theta} + \frac{\partial c}{\partial \zeta} = \frac{1}{N_{Pe}} \frac{\partial^2 c}{\partial \zeta^2} \tag{A-1}$$

Introduction of a new dependent variable

$$Z = c \exp - k\theta$$

yields a transformed differential equation

$$\frac{\partial^2 Z}{\partial \zeta^2} + N_{Pe} \frac{\partial Z}{\partial \zeta} - N_{Pe} \frac{\partial Z}{\partial \theta} - N_{Pe} Z = 0 \tag{A-2}$$

which, when Laplace transformed with respect to θ, gives

$$\frac{d^2 \overline{Z}}{d\zeta^2} - N_{Pe} \frac{d\overline{Z}}{d\zeta} - N_{Pe} (s + k) \overline{Z} = 0 \tag{A-3}$$

where $\overline{Z}$ is the Laplace transform of Z. By requiring $\overline{Z}$ to be bounded at $\zeta = \infty$, the solution, in the domain of the transformed variable s, of Equation (A-3) becomes

$$\overline{Z}(\zeta, s) = \overline{Z}(o, s) \exp \left[\frac{N_{Pe} - \sqrt{N^2_{Pe} + 4N_{Pe}(s + k)}}{2} \zeta \right] \tag{A-4}$$

where $\overline{Z}(\zeta, s)$ and $\overline{Z}(o, s)$ are the Laplace transforms of the Z functions at ζ and 0, respectively, that is

$$\overline{Z}(\zeta, s) = \int_o^\infty Z(\zeta, \theta) \exp - \zeta\theta \, d\theta \tag{A-5}$$

Regarding the exponential function as being replaced by its series expansion

$$\overline{Z}(\zeta, s) = \int_o^\infty Z(\zeta, \theta) \left[1 - s\theta + \frac{s^2\theta^2}{2!} - \frac{s^3\theta^3}{3!} + \ldots \right] d\theta \tag{A-6}$$

one sees that, purely formally

$$\left. \frac{\partial^n \overline{Z}}{\partial s^n} \right]_{s=0} = (-1)^n \int_o^\infty Z(\zeta, \theta) \theta^n \, d\theta \tag{A-7}$$

Thus the moments of the Z function are related to the derivatives with respect to s of the transformed variable $\overline{Z}$ evaluated at $s = 0$.

In considering Equation (A-4) the downstream or outlet pulse is at $\zeta = 1$, or

$$0(s) = \overline{Z}(1, s) \tag{A-8}$$

and the inlet pulse is at $\zeta = 0$, or

$$I(s) = \overline{Z}(0, s) \tag{A-9}$$

With these notation changes, Equation (A-4) becomes

$$0(s) = I(s) \, T(s) \tag{A-10}$$

where

$$T(s) = \exp \frac{N_{Pe} - \sqrt{N^2_{Pe} + 4N_{Pe}(s + k)}}{2} \tag{A-11}$$

From Equation (A-10)

$$0(o) = I(o) \, T(o) \tag{A-12}$$

and

$$0'(o) = I(o) \, T'(o) + I'(o) \, T(o) \tag{A-13}$$

From Equation (A-7)

$$0(o) = \int_o^\infty Z(\theta) \, d\theta$$

$$= \int_o^\infty c_o(\theta) \exp - k\theta \, d\theta$$

$$= \int_o^\infty c_o(t) \exp - \frac{k}{\tau} t \frac{1}{\tau} dt$$

$$= \frac{1}{\tau} \int_o^\infty c_o(t) \exp - k't \, dt = \frac{1}{\tau} \alpha_o \qquad (A\text{-}14)$$

where

$$k' = \frac{k}{\tau} \qquad (A\text{-}15)$$

Similarly

$$I(o) = \frac{1}{\tau} \int_o^\infty c_i(t) \exp - k't \, dt = \frac{1}{\tau} \alpha_i \qquad (A\text{-}16)$$

$$0'(o) = \frac{1}{\tau^2} \int_o^\infty t \, c_o(t) \exp - k't \, dt = \frac{1}{\tau^2} \beta_o \qquad (A\text{-}17)$$

$$I'(o) = \frac{1}{\tau^2} \int_o^\infty t \, c_i(t) \exp - k't \, dt = \frac{1}{\tau^2} \beta_i \qquad (A\text{-}18)$$

From Equation (A-11)

$$T(o) = \exp \frac{N_{Pe} - \sqrt{N^2_{Pe} + 4N_{Pe} k'\tau}}{2} \qquad (A\text{-}19)$$

$$T'(o) = \frac{N_{Pe}}{\sqrt{N^2_{Pe} + 4N_{Pe} k'\tau}} \exp \frac{N_{Pe} - \sqrt{N^2_{Pe} + 4N_{Pe} k'\tau}}{2} \qquad (A\text{-}20)$$

By substituting (A-14), (A-16), and (A-19) into (A-12), there results

$$A = \frac{\alpha_o}{\alpha_i} = \exp \frac{N_{Pe} - \sqrt{N^2_{Pe} + 4N_{Pe} k'\tau}}{2} \qquad (A\text{-}21)$$

and by substituting appropriately into (A-13), there results

$$B = \frac{\beta_o}{\alpha_o} - \frac{\beta_i}{\alpha_i} = \frac{\tau N_{Pe}}{\sqrt{N^2_{Pe} + 4N_{Pe} k'\tau}} \qquad (A\text{-}22)$$

By solving (A-21) and (A-22) simultaneously for τ and N_{Pe}, one obtains

$$\tau = \frac{2B \ln A}{2 \ln A + 4Bk} \qquad (A\text{-}23)$$

$$N_{Pe} = \frac{2 \ln A}{1 - \frac{\tau}{B}} \qquad (A\text{-}24)$$

Thus, to compute τ and N_{Pe} from the data one computes the zeroth and first moments of the modified function $c \exp - k'\tau$ at each of the measurement points. One then computes A and B according to Equations (A-21) and (A-22) and then τ and N_{Pe} from Equations (A-23) and (A-24).

Manuscript received January 24, 1966; revision received May 18, 1966; paper accepted May 20, 1966.

Interfacial Turbulence During the Absorption of Carbon Dioxide into Monoethanolamine

P. L. T. BRIAN, J. E. VIVIAN, and D. C. MATIATOS

Massachusetts Institute of Technology, Cambridge, Massachusetts

Severe discrepancies exist between theoretical considerations and the carbon dioxide–monoethanolamine absorption data available in the literature. By desorbing the inert tracer propylene simultaneously with the absorption of carbon dioxide into monoethanolamine in a short wetted-wall column, it is shown that the physical mass transfer coefficient is increased substantially by the carbon dioxide–monoethanolamine chemical absorption process. This is presumably due to interfacial turbulence driven by surface tension gradients. The use of the actual physical mass transfer coefficient prevailing during carbon dioxide absorption into monoethanolamine results in a considerable improvement in the agreement between the penetration theory solution and the experimental data on the rate of absorption of carbon dioxide into monoethanolamine.

During the past twenty years a considerable amount of research has been directed toward understanding the effect of a simultaneous liquid phase chemical reaction upon the rate of gas absorption. Theoretical studies have been based upon the use of idealized models of the absorption process, and the differential equations describing these models have been solved for various types of chemical reaction mechanisms and reaction kinetic equations. These theoretical studies have been supplemented by a number of experimental investigations with the use of laboratory absorbers, such as the short wetted-wall column and the laminar liquid jet, in which the interfacial area is known accurately and in which physical absorption rates have been shown to agree closely with penetration theory predictions.

In a few instances, encouraging quantitative agreement has been achieved between the theoretical predictions and the experimental measurements of the rate of gas absorption accompanied by a simultaneous chemical reaction. There have, however, been a number of disturb-